

Elderly human thoracic FE model development and validation

Atsutaka Tamura

Isao Watanabe

Kazuo Miki

Toyota Central R&D Labs., Inc.

Japan

Paper Number: 05-0229

ABSTRACT

Blunt impact to the anterior chest during frontal crash often causes sternum and rib fractures. In particular, several studies have reported that elderly people are susceptible to the complications following bony fractures mainly in the thoracic region, thereby, leading to high mortality and morbidity rates. These fractures are attributable to the reduced bone strength due to age-related osteoporosis. In this study, the authors developed a human thoracic FE model of the elderly occupant based on the 50th percentile male model, THUMS[®] (Total HUMAN Model for Safety) and the dynamic chest responses were validated during compression against experimental test data using post-mortem human subject (PMHS) specimens under realistic loading conditions that would be experienced by vehicular occupants restrained by an air bag and a seat belt.

INTRODUCTION

Highly energetic, trauma-like traffic accidents result in a high rate of morbidity and mortality. In particular, fractures of the bony thorax are the most frequent lesions in traumatic thoracic injury, while respiratory diseases such as pneumonia, flail chest, and pneumo/hemothorax are regarded as the leading complications associated with sternum and multiple rib fractures. Moreover, elderly people have a decreased injury tolerance due to the deteriorated bone strength related to osteoporosis and have been found to have a higher risk of fatal outcomes (AIS 3+). Thus, chest trauma, to the elderly people which involves bony fractures of the thoracic region, is associated with life-threatening complications despite its lower AIS value, which is an index of threat-to-life due to a specific injury (Bergeron et al., 2003; Bulger et al., 2000; Mayberry et al., 1997; Morris et al., 2002; Segers et al., 2001; Ziegler et al., 1994).

In industrialized countries, it is expected that by the year 2025 approximately 22% of the population will comprise people aged 60 years and above. For

instance, the population aged 65 years and older has been increasing in the U.S., and it is expected to make up more than 20% of the total U.S. population by the year 2030 (Dejeammes et al., 1996; Stutts et al., 1989). On the basis of computed crash rates using an estimate of annual mileage (i.e., crash rates per estimated million vehicle miles), the involvement of older drivers in crashes is greater than that of the overall population, although the percentage increases in the older age group are not as great as in the total licensed driver population (Stutts et al., 1989). Similarly, Shimamura et al. (2003) reported that in Japan, the percentage of elderly people aged 65 years and above reached 17.3% of the total population in the year 2000. They also analyzed the relationship between age groups and chest injury severity using a database of 246 belted occupants that were collected from 1993 to 2000 by ITARDA (Institute for Traffic Accident Research and Data Analysis) in Japan, and clarified that the injury severity in the elderly is closely related with the occurrence of multiple rib fractures. As described above, concerns about the growing transportation needs of the elderly and the necessity to make the traffic environment safer for older drivers arise from the potential risk of high injury rates related to motor vehicle accidents (Dellinger et al., 2002; Sjögren et al., 1993). These concerns are of importance particularly in light of the increase in life expectancy and rise in the proportion of elderly people in the population.

Meanwhile, Cesari et al. (1994) loaded the chests of volunteers, Hybrid III dummies, and human cadavers using a diagonal belt and found out that the location of maximum chest deflection was observed at points other than the mid-sternum. Furthermore, Morgan et al. (1996) investigated separate injury criteria for localized (*belt-like*) and distributed (*bag-like*) loading categories based on the normalized chest deflection and maximum chest acceleration and stated that the belt-only restraint system generally had a higher thoracic injury rate than the air bag-only restraint system. Recently, King (2000) reviewed previous studies on human tolerance to blunt impact and summarized the biomechanical knowledge of traumatic head, neck, and thorax injury. In this review article, King cited that the current injury

criterion prescribed in FMVSS 208 on chest compression of 76 mm is based on a recommendation by Neathery et al. (1973), who analyzed Kroell's data (1994) on blunt impact to the human thorax with a cylindrical rigid impactor to develop the thoracic response corridor. However, when the thorax was subjected to such a blunt impact and the force-deflection relationship was measured at the impacted area, a large inertial force would have been measured prior to the occurrence of the significant deformation of thorax observed. As a result, the characteristics of the thoracic response might be severely dominated by the inertial effect as noted by Kent et al. (2003b). Additionally, as stated earlier, vehicular occupants today are more likely to be restrained by a 3-point belt and air bags; therefore, the injury pattern during frontal crashes has altered due to the increased availability of safety devices. This raises the question of whether it is possible to evaluate the thoracic injury under any realistic loading condition using the injury risk function with this deflection-dependent criterion alone. In response to this, Kent et al. (2003b) designed a series of chest compression tests using human cadaveric specimens to study the effective stiffness of the thorax at a realistic loading rate under four loading conditions. They elucidated that the highest effective thoracic stiffness was measured with a distributed loading, followed by a double diagonal (4-point) belt, diagonal belt, and rigid hub depending on the difference in the loaded area and the interaction with the clavicles.

The purpose of the present study is to develop a thoracic FE model for elderly occupants and investigate the validity of its responses and potential injury patterns under realistic loading environments in a frontal crash.

METHODS

Small specimen test

First, material properties of the cortical rib in an elderly male were determined based on experimental test data obtained by Stitzel et al. (2003) at Virginia Technical University. They performed a dynamic 3-point bending test using small cortical bone samples obtained from the exterior surface of the ribs of human cadaver subjects whose ages ranged between 61 and 67 years (2 males). A total of 23 specimens were procured (6 specimens from the anterior part, 10 specimens from the lateral part, and 7 specimens from the posterior part) per cadaver, and each specimen was subjected to a 3-point bending load dynamically at the rate of ~5 strain/s. Specifically, as shown in Figure 1, a small specimen (24.0 mm in length \times 7.0 mm in

width \times 0.6 mm in thickness) was simply supported at both ends, and the impactor was prescribed to move at 365 mm/s to compress the middle point of a small specimen as per the ASTM Standard D790-00. The bending load for all specimens was applied in an exterior to interior direction relative to the in situ anatomy of the rib. This setup was considered to be a realistic loading condition produced by the seat belt and air bag, with the exception of the lateral part of the rib specimens, which was assumed to be bent from the interior to the exterior direction with compressive load from the anterior chest. According to their report, the strength and stiffness of the cortical rib greatly varied depending on the location and rib level in the human rib cage, and the anterior segment of the cortical rib was found to be weaker than the posterior segment, which is also weaker than that of the lateral rib. In the present study, however, the rib section was simply divided into 3 parts – anterior part, lateral part, and posterior part – and the material strength of the cortical rib was given by averaging the experimental test data obtained from each rib segment so that the difference in the material property of the cortical rib can be clearly considered in the simulation model.

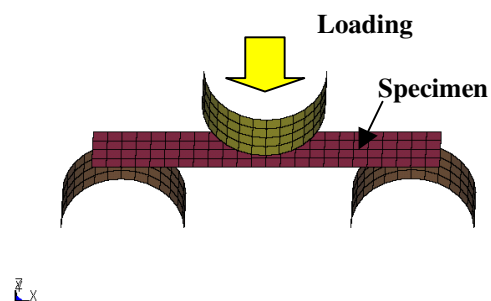


Figure 1: Dynamic 3-point bending test simulation for a small cortical rib specimen

Chest compression test

Second, model responses to the dynamic chest compression were validated against the experimental test data obtained by Kent et al. (2003b) at the University of Virginia (UVA). The human cadavers used in the test were aged between 75 and 79 years. They performed a series of chest compression tests with PMHS specimens positioned with their spine on a rigid table and the slave cylinder was prescribed to translate into a step rise time of 50 ms at a displacement rate of ~1.0 m/s (Figure 2a, b). This is similar to the chest deflection rate of the occupants restrained by a seat belt in a frontal crash while traveling at 48 km/h. In the experimental test setup, the chest deflection was measured anteriorly at the mid-sternum point, while the reaction force was measured posteriorly using the load cell placed behind each subject's back. In reality, however, this type of

loading condition cannot be expected for vehicular occupants since their back is normally free in the compartment, and no reaction force is generated in the posteroanterior direction in a frontal crash. In the present study, data from three elderly cadaver subjects who had undergone dynamic chest compression was compared with the simulation results using distributed, hub, diagonal belt, and 4-point belt loading conditions as shown in Figures 3a–d. Specifically, a 20.3 cm wide band was used to compress the area between the second and seventh ribs for distributed loading, while a 15.2 cm diameter circular plate was used for hub loading to mimic the loading surface described by

Kroell et al. (1994). In addition, a 5.0 cm wide belt was used to pass over the shoulder to the lower ribs of the PMHS specimens for diagonal belt and 4-point belt loading. In these simulations, only gravity was applied for an initial 120 ms prior to dynamic compression of the thorax so that the stable condition would be obtained for determining a zero point in force-deflection curves. It should be noted that in this series of experimental tests, the generation of bone fracture was not attempted by impacting the thoracic region. Finally, we conducted an injury analysis up to the bone fracture level by compressing the thoracic region at a rate of 0.6 m/s.

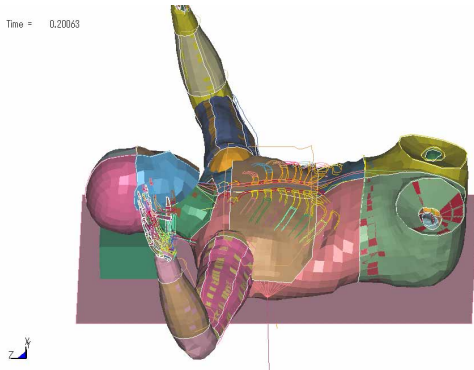


Figure 2a: Simulation setup[#]
[#][Chest is compressed by distributed loading.]

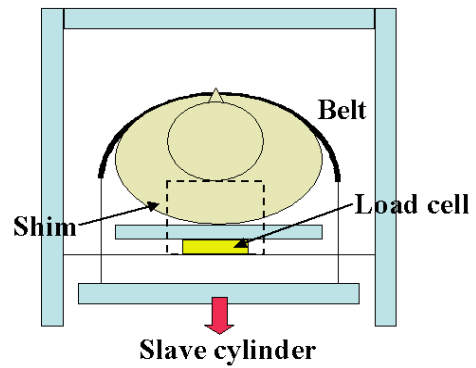


Figure 2b: Test setup for dynamic chest compression via loading cable conducted at UVA

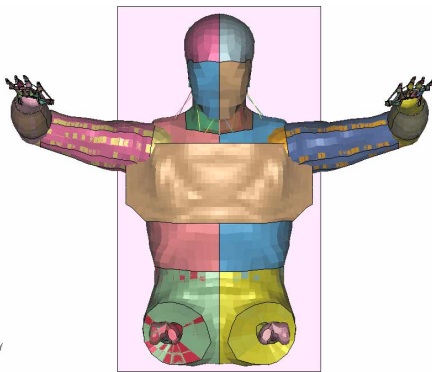


Figure 3a: Initial condition for distributed loading

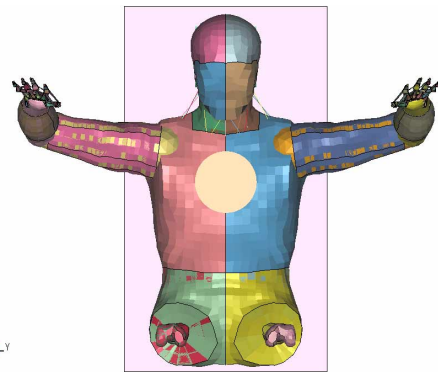


Figure 3b: Initial condition for hub loading

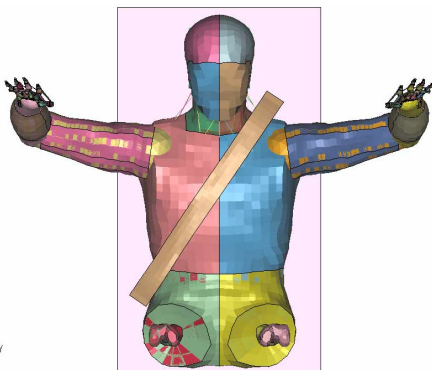


Figure 3c: Initial condition for diagonal belt loading

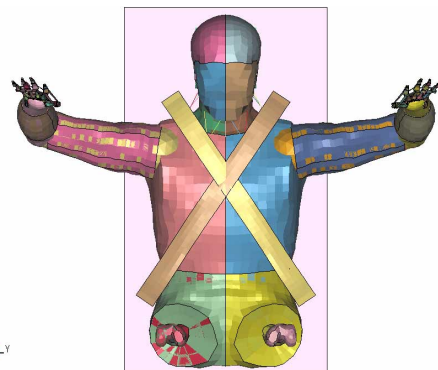


Figure 3d: Initial condition for 4-point belt loading

RESULTS

Small specimen test

First, on the basis of the experimental test results (Stitzel et al., 2003), the material property of the cortical rib in an elderly male was determined as summarized in Table 1 by means of the elastic beam theory, while simulation results using small specimens were compared with those of the experimental tests as shown in Figure 4. In this section, the yield point was defined by averaging the real yield points in each

force-deflection plot by 0.1% offset strain strength. Since the force-deflection responses in cortical rib bending tests were greatly dispersed, material coefficients such as the Young's modulus and plastic tangent modulus were also determined by averaging the experimental test data so that the calculated results would exist within the force-deflection responses. In addition, the ultimate tensile strain was defined as 0.020 (2.0%) in view of the reduced bone strength with aging (Lindahl et al., 1967; McCalden et al., 1993).

Table 1: Material property of the cortical rib in an elderly male[†]

	σ_y (MPa)	ϵ_y	YM (GPa)	Etan (GPa)	ϵ_p	ϵ_{max}
Anterior part	121.6	0.0145	8.394	3.792	0.0055	0.020
Lateral part	135.3	0.0111	12.211	4.610	0.0089	0.020
Posterior part	112.9	0.0103	10.998	6.332	0.0097	0.020

[[†] σ_y : yield stress, ϵ_y : yield strain, YM: Young's modulus, Etan: plastic hardening modulus, ϵ_p : plastic strain, ϵ_{max} : ultimate strain]

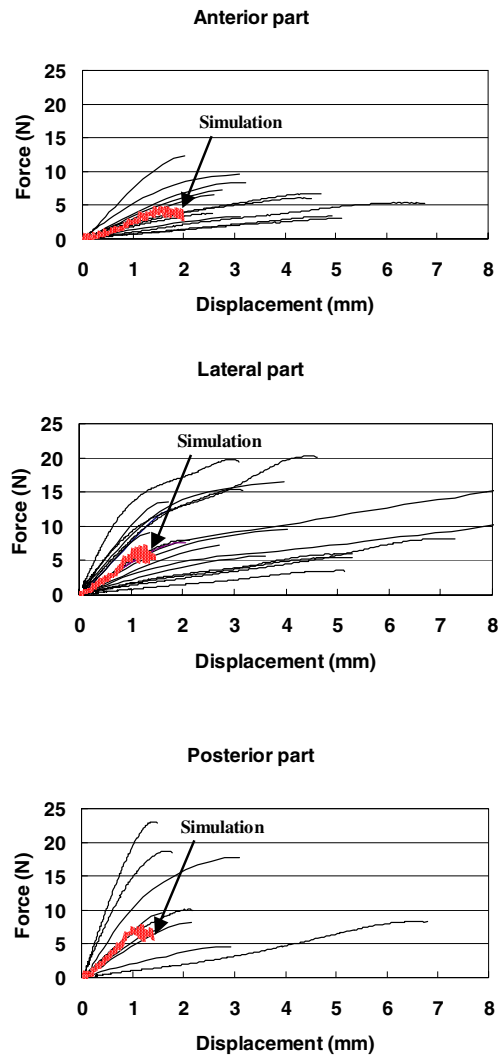


Figure 4: 3-point bending test results using rib cortical specimens

Chest compression test

Second, the calculated result with respect to the thoracic part was validated against laboratory test data obtained by Kent et al. (2003b) using human cadaver subjects. As demonstrated in Figure 5, the calculated thoracic responses to dynamic chest compression are almost identical with the experimental results, and thoracic stiffness was found to be greatly dependent on

the interaction between the clavicles and the 1st ribs as well as the magnitude of the loaded area due to compressing devices. Additionally, as it can be seen in a frontal crash with air bag deployment, stress concentration was observed at the lateral part of the rib cage under distributed loading condition (Crandall et al., 2000; Yoganandan et al., 1996). Meanwhile, for hub loading, stress concentration was only observed at the sternum level.

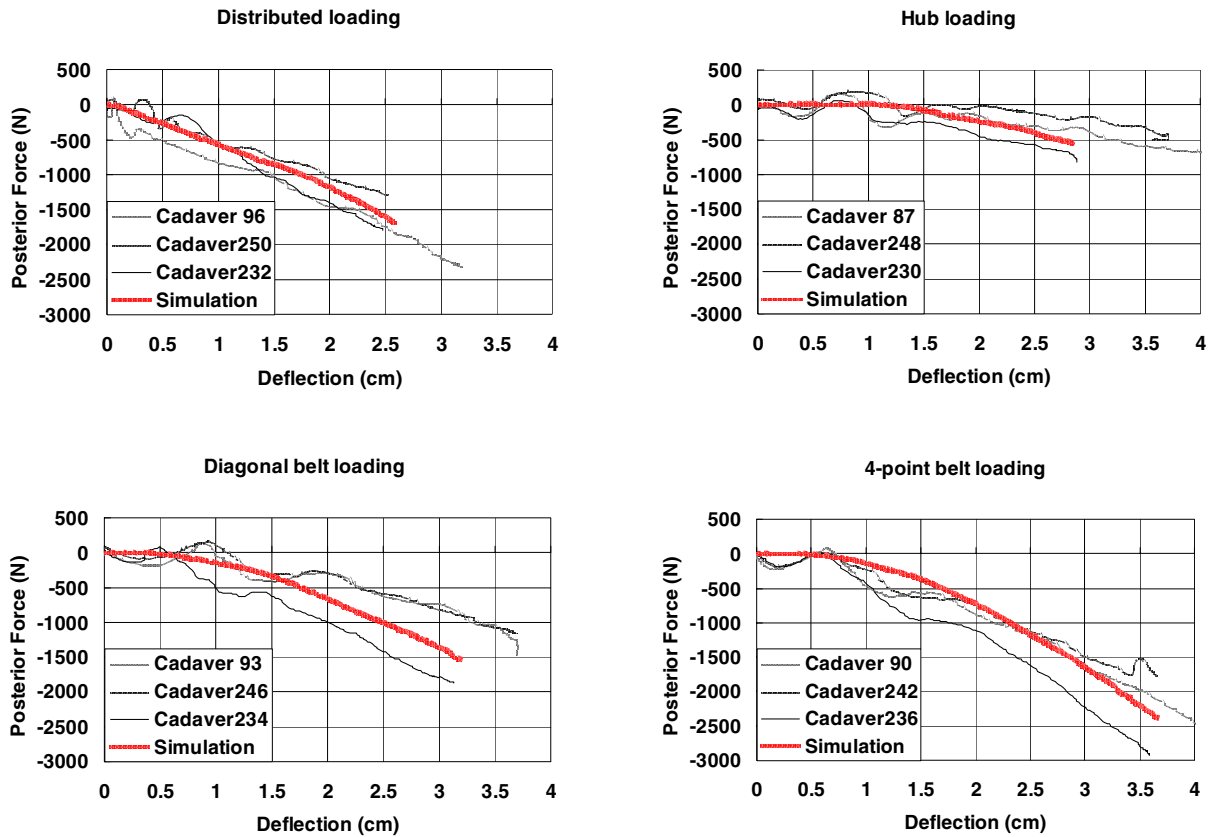
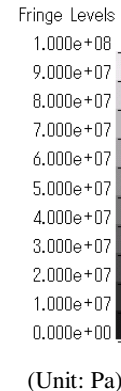


Figure 5: Force-deflection responses in chest compression under four loading environments

Injury analysis

Finally, we investigated thoracic hard tissue failure patterns due to excessive anterior chest compression. The same test setups were used as those employed in the previous section. Hence, a series of FE simulations were subsequently conducted, and the element elimination technique was used to assess the bone fractures of the sternum and the rib cortical bone. As illustrated in Figures 6a–d, multiple hard tissue failures and various fracture patterns were predicted around compressing devices except for the 4-point belt and fracture timing was also tracked (Figures 7a–d). Although no bone fracture was observed against 4-point belt loading, as stated earlier, considerable stress concentrations were observed at several locations in the

clavicles and the lateral part of the rib cage, as shown in Figure 6d.



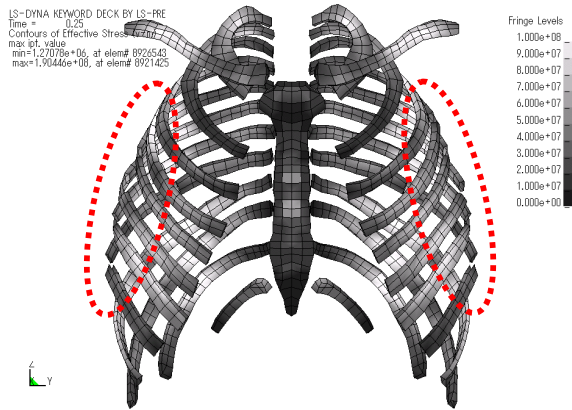


Figure 6a: Equivalent stress distribution by distributed loading (at 120 ms)*

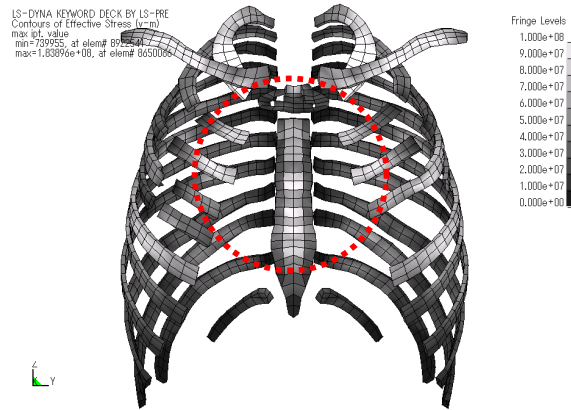


Figure 6b: Equivalent stress distribution by hub loading (at 157 ms)*

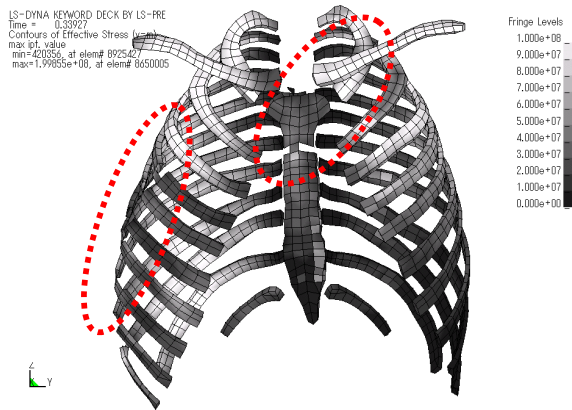


Figure 6c: Equivalent stress distribution by diagonal belt loading (at 210 ms)*

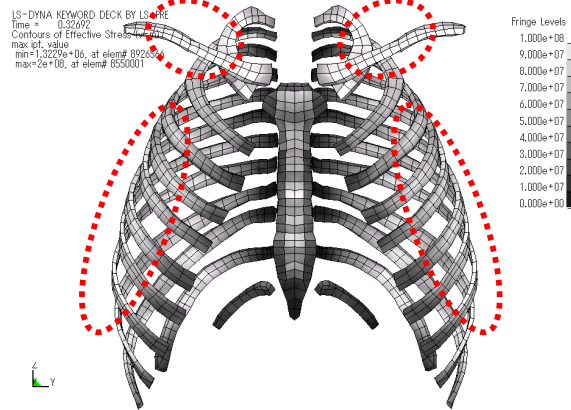


Figure 6d: Equivalent stress distribution by 4-point belt loading (at 197 ms)*

[*Enclosed area with dotted line corresponds to the area of stress concentration.]

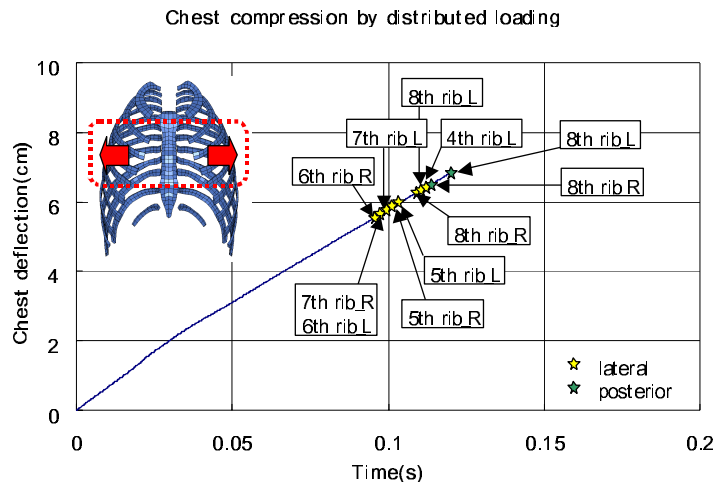


Figure 7a: Time history of chest deflection and fracture timing due to distributed loading[‡]

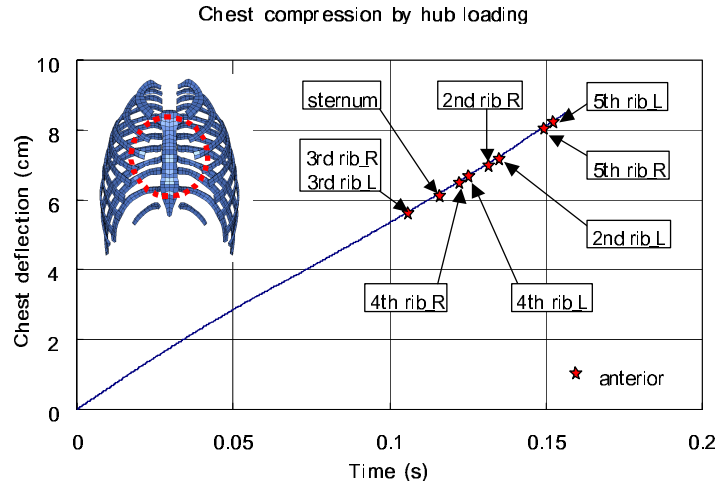


Figure 7b: Time history of chest deflection and fracture timing due to hub loading[‡]

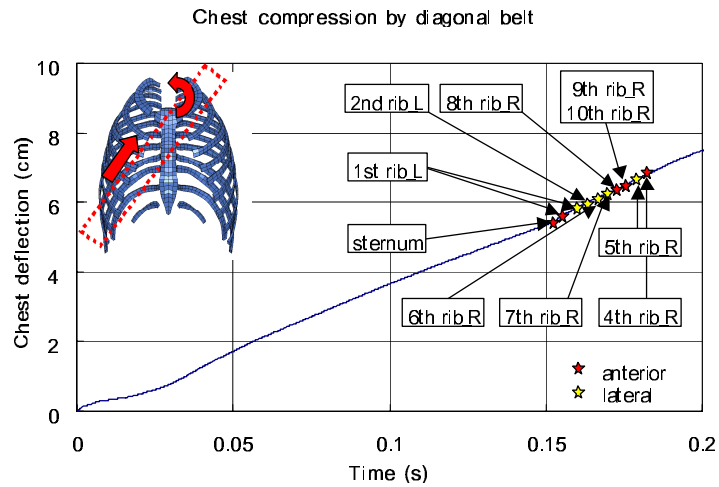


Figure 7c: Time history of chest deflection and fracture timing due to diagonal belt loading[‡]

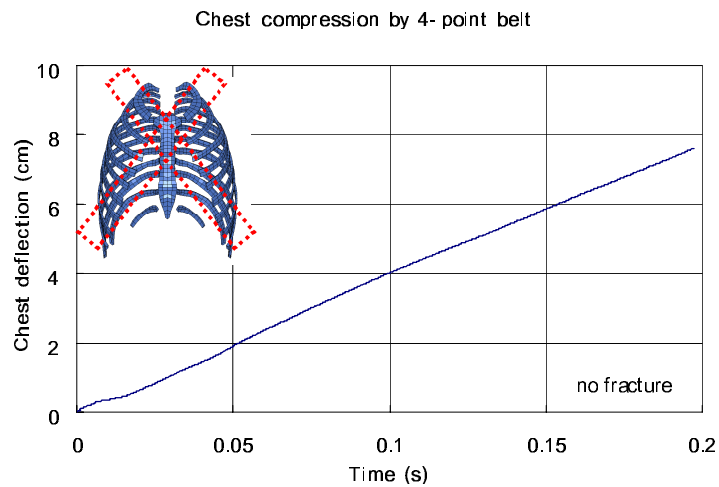


Figure 7d: Time history of chest deflection and fracture timing due to 4-point belt loading[‡]
[‡]R indicates right ribs, and L indicates left ribs.]

DISCUSSION

Small specimen test

The mechanical property of the cortical rib was determined based on the experimental test results. In general, the ultimate tensile strain as an index of bone strength is considered to gradually reduce with aging. In other words, the mechanical property of cortical bones in the elderly is believed to be relatively close to that of a brittle material rather than an elasto-plastic material. Whereas, by dynamically conducting a 3-point bending test, Stitzel et al. (2003) found that the plastic region of the cortical rib in the elderly is much greater than expected, although material property varies considerably depending on its location and rib level. According to their results, some of the small specimens subjected to a dynamic bending load demonstrated a large tensile strain in excess of 0.080 (8.0%) on the lower surface of the specimens. In the present study, however, ultimate strain was determined as 0.020 (2.0%). This was based on previous studies in which the material property of the cortical bone was experimentally investigated using humeral and femoral coupons in pure tension (Lindahl et al., 1967; McCalden et al., 1993) so that the effect of reduced bone strength with aging can be clearly taken into account. When the elastic beam theory is employed to derive the mechanical property of the cortical rib, the relationship between stress and strain can be calculated based on the assumption that its distribution in the loaded section is ideally symmetrical with respect to the neutral axis. However, this assumption may not be acceptable for large deflections occurring due to excessive bending load, and the behavior post-yield point can no longer be estimated correctly. Nevertheless, the authors will support their test method at this stage because of the difficulty in the existing experimental measuring technique. Further, we believe that the 3-point bending test is still one of the best ways to obtain the mechanical property of the cortical rib against such a high speed impact. This is because such a bending load is regarded to be a dominant factor in causing hard tissue failure of the thorax in a restrained vehicular occupant in frontal crashes.

Chest compression test

The model was then validated against the dynamic thoracic compression tests under four realistic loading conditions. It may be difficult to compare the results obtained here to Kroell's test results (1994) using a rigid impactor, which might be dominated by the inertial effect, because PMHS specimens in this study

were laid along the spine position on a rigid table, and the reaction force was measured posteriorly to derive the effective thoracic stiffness. Therefore, as stated earlier, the authors initially applied only gravity on the model lying on a rigid table in order to obtain a stable condition prior to dynamically compressing the anterior chest. In addition, the material property of the deformable solid elements used as a substitute for internal organs inside the thoracic cavity was adjusted so that it would respond against impacting load in a manner similar to a pressurized lung by means of the preliminary test results obtained at our laboratory (Hayamizu et al., 2003) since Kent et al. (2003b) also pressurized the pulmonary system to model the in vivo condition as much as practically possible before conducting a series of chest compression tests. Although we had paid careful attention to reconstruct the boundary conditions of the experimental test setup, the difference observed in force-deflection responses between simulation and experimental test results might be responsible for a mismatch in its boundary condition or the effect of the internal organ, which are not included in the current THUMS model (Oshita et al., 2001). Nonetheless, we believe that our results showed reasonable responses compared to the experimental test results in view of the general trend observed when subjected to realistic dynamic chest compression. Further, this model can be applied for practical problems such as a frontal crash simulation. However, since rib fracture is suspected to lacerate the internal organs and its injury mechanism remains unknown, we need to develop and integrate a detailed internal organ model so that visceral injury as well as thoracic bony failures can be predicted.

Injury analysis

In this section, the rib cortical bone was subjected to a severe bending load from the anterior chest at a relatively slow loading rate, as mentioned earlier. However, the authors are concerned about the possible overestimation of the magnitude of its ultimate stress strength in the model due to the theoretical approach of the elastic beam theory employed in the present study. Additionally, material property of flesh (soft tissue) remains unclear, although it is believed to be crucial for estimating the probability of chest injury since flesh tissue is considered to be effectively distributing the load from the anterior chest (Kent et al., 2001).

In summary, we have found the following results under these four loading environments:

- 1) **Distributed loading:** Bone fracture was predicted to propagate from the lateral side to the posterior

side as such a fracture pattern could be expected for typical air bag loading.

- 2) **Hub loading:** Bone fracture was only predicted around the anterior chest due to the excessive bending load on the anterior surface of the thorax.
- 3) **Diagonal belt loading:** Bone fracture was predicted in the inferior to superior direction along the path of a diagonal belt. It was also observed that the anterior part of the thorax failed due to sternum torsion and the interaction between the clavicle and the 1st rib.
- 4) **4-point belt loading:** Although bone fracture was not predicted in this case, considerable stress concentrations were observed at several locations for both the clavicles and the lateral part of the rib cage. Since the rate of compression was set to be relatively moderate in comparison with a real loading environment, intrinsic symmetry stemming from such a 4-point belt appears to sufficiently distribute the total load over the rib cage.

In the present study, the chest deflection of 70 mm corresponds to the thoracic compressive ratio of 32.5% for the current chest depth of THUMS. According to the analytical results reported by Kent et al. (2003a), the probability of injury risk for $fx. > 6$ (greater than six rib fractures) can be estimated to be over 50% for elderly people aged 70 years old with the ratio of 32.5% chest compression. Although four types of restraint conditions were employed in this section, the onset of fracture timing was almost similar except in the case of 4-point belt loading. Specifically, the fracture onset was observed at a magnitude of 50 mm chest deflection, and multiple bone fractures ($fx. > 6$) were observed at a magnitude of 70 mm chest deflection. However, most of the stress concentration was observed along the path of the diagonal belt line as well as the lateral part of the rib cage due to excessive bending load from the anterior chest. In particular, stress concentration was observed at the lower part of the rib cage rather than at the mid-sternum level. Despite the fact that the magnitude of chest deflection is evaluated at the mid-sternum level for the current crash test dummy, it is inconclusive as yet whether maximum chest compression (C_{max}) is always suitable for chest injury prediction. Thus, the possibility that the current chest compression criterion based on the mid-sternum level alone would be a sufficient index for predicting injury risk is still open to discussion as suggested by the previous studies (Cesari et al., 1994; Morgan et al., 1996). Future studies should integrate this thoracic model for the elderly with THUMS and apply it for frontal crash simulation in combination with a seat belt and air bag loading to investigate the

effect on the protection and safety of the occupant as shown in Figure 8.



Figure 8: Sled test model with a belted occupant

CONCLUSION

Thoracic part of the elderly male occupant was developed based on Total HUMAN Model for Safety (THUMS®) so that it would be applied for predicting thoracic hard tissue injury by taking into account the decreased bone strength due to aging. Now we hope that the thoracic characteristics of an elderly occupant obtained from the present study will be applied to more realistic cases in order to advance the safety protection performance of the current restraint system.

ACKNOWLEDGMENTS

The authors greatly acknowledge the contribution of Wayne State University for the development of the head and thorax part of THUMS. We also wish to thank the University of Virginia and Virginia Technical University for their sincere support and assistance under the contract of collaborative research program with Toyota Motor Corporation (2002-2003). In addition, the authors thank Mr. Junji Hasegawa and Mr. Fumio Matsuoka of Toyota Motor Corporation who have provided us with a valuable advice and comments to complete this study.

REFERENCES

- Bergeron, E., Lavoie, A., Clas, D., Moore L., Ratte, S., Tetreault, S., Lemaire, J., Martin, M. (2003); "Elderly trauma patients with rib fractures are at greater risk of death and pneumonia", *J. Trauma*, Vol. 54, pp. 478-485.
- Bulger, E. M., Arneson, M. A., Mock, C. N., Jurkovich, G. J. (2000); "Rib fractures in the elderly", *J. Trauma*, Vol. 48, pp. 1040-1047.
- Cesari, D., Bouquet, R. (1994); "Comparison of hybrid III and human cadaver thorax deformations loaded by

- a thoracic belt”, In Proc. of 38th Stapp Car Crash Conf., pp. 65-76, SAE# 942209.
- Crandall, J. R., Kent, R., Patrie, J., Fertile, J., Martin, P. (2000); “Rib fracture patterns and radiologic detection – A restraint-based comparison”, In Proc. of Annual Proceedings of 44th Association for the Advancement of Automotive Medicine, pp. 235-259.
- Dejeammes, M., Ramet, M. (1996); “Aging process and safety enhancement of car occupants”, In Proc. of 15th International Technical Conf. on Enhanced Safety Vehicles, pp. 1189-1196.
- Dellinger, A. M., Langlois, J. A., Li, G. (2002); “Fatal crashes among older drivers: Decomposition of rates into contributing factors”, American Journal of Epidemiology, Vol. 155, pp. 234-241.
- Hayamizu, N., Watanabe, I., Ishihara, T., Miki, K. (2003); “Measurement of impact response of pig lung”, In Proc. of JSME Tokai Branch Conf., pp. 94-95. (in Japanese)
- Kent, R., Crandall, J. R., Bolton, J., Prasad, P., Nusholtz, G., Mertz, H. J. (2001); “The influence of superficial soft tissues and restraint condition on thoracic skeletal injury prediction”, Stapp Car Crash Journal, Vol. 45, pp. 183-204.
- Kent, R., Patrie, J., Poteau, F., Matsuoka, F., Mullen, C. (2003a); “Development of an age-dependent thoracic injury criterion for frontal impact restraint loading”, In Proc. of 18th International Technical Conf. on Enhanced Safety of Vehicles.
- Kent, R., Sherwood, C., Lessley, D., Overby, B., Matsuoka, F. (2003b); “Age-related changes in the effective stiffness of the human thorax using four loading conditions”, In Proc. of International Research Council on the Biomechanics of Impact.
- King, A. I. (2000); “Fundamentals of impact biomechanics Part 1 --- Biomechanics of the head, neck and thorax”, Annu. Rev. Biomed. Eng., Vol. 2, pp. 55-81.
- Kroell, C. K. (1994); “Thoracic response to blunt frontal loading”, In Biomechanics of impact injury and injury tolerances of the thorax-shoulder complex (Backaitis, S.H., ed.), pp. 51-79, SAE, Inc.
- Lindahl, O., Lindgren, Å. G. H. (1967); “Cortical bone in man II. Variation in tensile strength with age and sex”, Acta Orthop. Scandinav., Vol. 38, pp. 141-147.
- Mayberry, J. C., Trunkey, D. D. (1997); “The fractured rib in chest wall trauma”, Chest Surg. Clin. N. Am., Vol. 7, pp. 239-261.
- McCalden, R. W., McGeough, J. A., Barker, M. B., Cout-Brown, C. M. (1993); “Age-related changes in the tensile properties of cortical bone”, J. Bone Joint Surg., Vol. 75, pp. 1193-1275.
- Morgan, R. M., Eppinger, R. H., Kuppa, S. M., Taylor, L. M. (1996); “Thoracic trauma assessment for the hybrid III dummy in simulated frontal crashes”, In Proc. of 15th International Technical Conf. on Enhanced Safety Vehicles, pp. 1605-1621.
- Morris, A., Welsh, R., Frampton, R., Charlton, J., Fildes, B. (2002); “An overview of requirements for the crash protection of older drivers”, In Proc. of Annual Proceedings of 46th Association for the Advancement of Automotive Medicine.
- Neathery, R. F., Lobdell, T. E. (1973); “Mechanical simulation of human thorax under impact”, SAE Technical Paper, pp. 451-466, SAE# 730982.
- Oshita, F., Omori, K., Nakahira, Y., Miki, K. (2001); “Development of a finite element model of the human body”, In Proc. of 7th Int. LS-Dyna Users Conf.
- Segers, P., Van Schil, P., Jorens, Ph., Van Den Brande, F. (2001); “Thoracic trauma: an analysis of 187 patients”, Acta. Chir. Belg., Vol. 101, pp. 272-282.
- Shimamura, M., Ohhashi, H., Yamazaki, M. (2003); “The effects of occupant age on patterns of rib fractures to belt-restrained drivers and front passengers in frontal crashes in Japan”, Stapp Car Crash Journal, Vol. 47, pp. 349-365.
- Sjögren, H., Björnstig, U., Eriksson, A., Sonntag-Öström, E., Öström, M. (1993); “Elderly in the traffic environment: Analysis of fatal crashes in northern Sweden”, Accid. Anal. & Prev., Vol. 25, pp. 177-188.
- Stitzel, J. D., Cormier, J. M., Barretta, J. T., Kennedy, E. A., Smith, E. P., Rath, A. L., Duma, S. M., Matsuoka, F. (2003); “Defining regional variation in the material properties of human rib cortical bone and its effect on fracture prediction”, Stapp Car Crash Journal, Vol. 47, pp. 243-265.
- Stutts, J. C., Waller P. F., Martell, C. (1989); “Older driver population and crash involvement trends, 1974-1986”, In Proc. of 33rd Annual Proceedings of Association for the Advancement of Automotive Medicine, pp. 137-152.
- Yoganandan, N., Morgan, R. M., Eppinger, R. H., Pintar, F. A., Sances, A. Jr., Williams, A. (1996); “Mechanisms of thoracic injury in frontal impact”, J. Biomechanical Eng., Vol. 118, pp. 595-597.
- Ziegler, D. W., Agarwal, N. N. (1994); “The morbidity and mortality of rib fractures”, J. Trauma, Vol. 37, pp. 975-979.